CHEMISTRY OF MATERIALS

Article

pubs.acs.org/cm

Solution-Dispersible, Colloidal, Conjugated Porous Polymer Networks with Entrapped Palladium Nanocrystals for Heterogeneous Catalysis of the Suzuki–Miyaura Coupling Reaction

Peng Zhang,[†,‡] Zhihuan Weng,[‡,§,⊥] Jia Guo,*[,†] and Changchun Wang[†]

[†]State Key Laboratory of Molecular Engineering of Polymers, Department of Macromolecular Science, Fudan University, Shanghai 200433, P. R. China

[§]Institute for Molecular Science, National Institute for Material Science, Okazaki 444-8787, Japan

Supporting Information

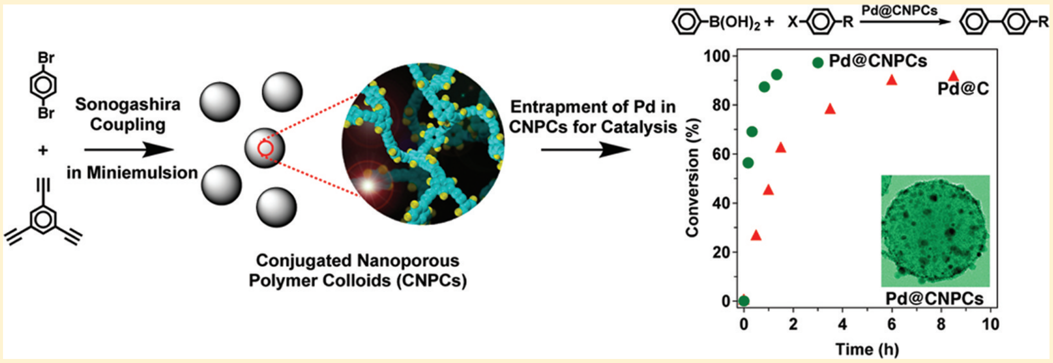

ABSTRACT: Conjugated nanoporous polymer colloids (CNPCs) consisting of covalently cross-linked poly(*p*-phenyleneethynylene) networks were synthesized by using the Sonogashira coupling reaction in a toluene-in-water miniemulsion. The synthesized CNPCs having a uniform particle size distribution exhibit high porosity with a specific surface area of 421 m^2/g and a dual distribution of pore size in the micropore and mesopore ranges. They are amenable to postfunctionalization and enhancement of their dispersibility in solvents, and retain their native photoluminescence. The modified CNPCs allow for in situ incorporation of palladium nanocrystals to form the Pd@CNPC composite materials. The Pd@CNPCs are validated to have excellent catalytic activity, outstanding reusability, and exceptionally high TOF (44100 h^{-1}) for the Suzuki–Miyaura coupling reaction.

KEYWORDS: *conjugated polymer networks, composite colloids, heterogeneous catalysis, nanoporosity, Pd nanocrystals*

INTRODUCTION

Conjugated microporous polymers (CMPs), which continue to attract increasing attention as a class of microporous organic polymers, have been proving to be invaluable tools in the fields of gas storage,[1] catalysis,[2] light harvesting,[3] and supercapacitive energy storage.[4] Because of their chemical diversity, CMPs have been thoroughly explored compared to other known microporous organic polymers, e.g., hyper-cross-linked polymers (HCPs),[5] polymers of intrinsic microporosity (PIMs),[6] and covalent organic frameworks (COFs).[7] To date, extensive research has led to rapid development in the synthesis of various CMPs.[8] These systems are greatly promising for advanced applications in organic electronics and luminescent sensors. To achieve this end, it is necessary to endow CMPs with solution properties to enable the fabrication of architectures such as coatings, films, or colloids. However, the cross-linked rigid skeletons of CMPs are insoluble and infusible, and retain monolithic morphologies during postmodification. Although studies on the development of processable microporous polyurea networks by an organic sol–gel strategy have recently been reported,[9] the micropore sizes obtained (<1 nm), as estimated by capture of CO_2, were unfortunately too small to allow nitrogen gas to freely permeate. Also, the conjugation of polyurea networks was broken by the urea moieties (–NHCONH–); therefore, the first unequivocal example of CMPs with suitable solution properties has yet to be reported.

CMPs as catalytic support are of distinct advantage over other known porous organic materials since they can serve as an ideal platform for chemically entrapping catalytic modules into highly stable, covalently cross-linked, conjugated polymer networks by taking advantage of their permanent porosity and the ability to tailor their compositions and properties at the molecular level. The introduction of catalytic moieties into CMPs has two main strategies. The first is the bottom-up approach by which the building blocks with catalytic function groups are applied directly to construct the polymer networks.

Received: August 4, 2011
Revised: November 1, 2011
Published: November 3, 2011

This allows the catalytically active sites to be embedded onto the pore wall and thus facilitates their homogeneous distribution through CMPs. Lin et al. utilized the functionalized monomers with Ru and Ir complexes to synthesize the photoactive microporous polyphenylene for the heterogeneous photocatalysis.[2b] Cooper et al. developed the bottom-up methodology to synthesize a series of metal-anchored microporous poly(aryleneethynylene) networks for reductive amination.[2c] Unlike the above-mentioned, the second strategy is to incorporate metal nanocrystals into CMPs via post treatment method. Thomas et al. immobilized the PVA-stabilized Pd nanocrystals onto the surface of covalent triazine frameworks,[10] or reduced the poly(thienylene arylene) network-loaded palladium salts for in situ incorporation of Pd nanocrystals into organic microporous polymer.[8e] For enhancing the metal−support interaction, Cooper et al. used supercritical CO_2 to encapsulate the Pd nanocrystals by decomposition of a CO_2-soluble Pd complex in CMP networks.[11] Despite the advent of pioneer studies, it is still rarely investigated because inferior dispersibility of metal nanocrystal/CMP composite materials largely restrict their diverse applications. Additionally, pore sizes imposed by CMPs are predominated in the micropore regime and thus in situ incorporation of metal nanocrystals into CMP networks appears to be rather challenging.

Herein, we report a template synthesis of conjugated nanoporous polymer colloids (CNPCs) based on a heterogeneous coupling reaction in an oil-in-water miniemulsion system. The colloidal conjugated networks thus obtained were regularly spherical, consisted of fully fused organic skeletons, and had inherent, locked-in, open nanopores. Of more significance, they were unique in that they were amenable to size-controllable synthesis and enhancement of their dispersibility in solvents, and retained their native photoluminescence; all of the features are not accessible with solid-state CMPs. Therefore, these systems may offer new possibilities in terms of enhanced performances in multiple disciplines, even for the usual applications known for high-surface-area materials. Of particular appeal to us is the possibility of complexing metal nanocrystals within the porous networks, in view of the fact that unsaturated bonds such as ethynylene or vinylene in conjugated polymers can be directly employed to form metal-complexed polymers.[12] Thus, we have embarked on an exploration of the possibility of synthesizing solution-dispersible CNPCs with embedded metal nanoparticles, and present here our initial study on the in situ incorporation of Pd nanocrystals within CNPCs with a view to obtaining highly efficient heterogeneous catalysts.

■ EXPERIMENTAL SECTION

Materials. 1,3,5-Triethynylbenzene, 1,4-dibromobenzene, and tetrakis-(triphenylphosphine)-palladium(0) were purchased from Alfa Aesar (US). Copper iodide, triethylamine, cetyltrimethylammonium bromide, and $Pd(OAc)_2$ were purchased from Aladdin (China). All reagents for the catalysis of the Suzuki coupling reaction were purchased from TCI (Japan).

Synthesis of CNPCs End-Capped with *N*-[2-(4-iodophenoxy)-ethyl]-*N,N*-dimethylamine. 1,3,5-Triethynyl benzene (150 mg, 1 mmol), 1,4-dibromobenzene (236 mg, 1 mmol), tetrakis-(triphenylphosphine)-palladium(0) (58 mg), and copper iodide (19 mg) were degassed using three evacuation-N_2-backfill cycles. A mixture of toluene (1.5 mL) and triethylamine (1.5 mL) was added and stirred until the solid dissolved completely. The yellow solution obtained was mixed with 30 mL of a 1% aqueous cetyltrimethylammonium bromide (CTAB) solution with a syringe. The mixture was ultrasonicated for 10 min (SONICS-750 with a tip operated at 75 W). The miniemulsion was heated to 70 °C, and stirred for 24 h under N_2. After reaction, the mixture was cooled to room temperature and the product was obtained by precipitation in methanol and thoroughly washed with methanol, acetone, and chloroform to remove the surfactants and any unreacted monomer or catalyst residues. The further purification was carried out by Soxhlet extraction from methanol for 24 h. The product was dried in vacuum for 12 h at 40 °C. (Yield, 92%). *N*-[2-(4-iodophenoxy)ethyl]-*N,N*-dimethyl amine synthesized as previously reported (see the Supporting Information) was used as end-capper to react with the residual alkyne bonds on the surface of CNPCs. The dried powder of CNPCs (200 mg) was redispersed in a mixture of toluene (25 mL) and triethylamine (1.5 mL), and mixed with tetrakis-(triphenylphosphine)-palladium(0) (50 mg), copper iodide (15 mg) and end-capper (291 mg, 1 mmol). The reaction was allowed to proceed for 24 h at 70 °C under N_2. After being cooled, the precipitates were filtered off, washed with methanol, acetone and chloroform, and dried in vacuum.

Synthesis of Pd@CNPCs. The end-capped CNPCs (230 mg) was dispersed in water (20 mL) and mixed with the acetone solution (5 mL) of $Pd(OAc)_2$ (70 mg). After stirring at 90 °C for 1 h, the reaction mixture was filtered off, washed with hot water and acetone, and dried in vacuum. To determine the loading amount of Pd nanocrystals, the obtained Pd@CNPCs (3 mg) was dispersed in 13 M nitric acid (5 mL) and the mixture was heated at 80 °C to dissolve completely. After being cooled to room temperature, the solution was diluted for measuring the amount of Pd by ICP.

General Procedure for the Suzuki Coupling Reaction by Using Pd@CNPCs. 1-Iodo-4-methylbenzene (1 mmol), phenylboronic acid (1.1 mmol), K_2CO_3 (1.5 mmol) and Pd@CNPCs (0.1 mol %) were added to 3 mL of DMF/H_2O mixture with a volume ratio of 1:1, and then the mixture was heated to 50 °C with stirring for the time indicated under N_2. After the completion of the reaction, the mixture was filtered to collect the catalyst for the next cycle. The organic phase in the filtrate was extracted with dichloromethane by twice, and dried over $MgSO_4$. Finally, quantitative and qualitative analysis of the product was conducted with GC and GC/MS. The leaching of Pd in each cycle also was monitored by ICP.

Characterization. Solid-state ^{13}C cross-polarization magic-angle spinning (CP/MAS) NMR spectrum was measured on a Varian Infinity plus 300WB spectrometer at a MAS rate of 5 kHz and a CP contact time of 1.4 ms. HR TEM was carried on a JEM-2010 transmission electron microscope at an acceleration voltage of 200 kV (JEOL, Japan). The sample was prepared by drop-casting an aqueous dispersion onto a copper grid. EDX spectrum was measured on the TEM instrument with an EDXS spectrometer. Nitrogen sorption measurements were collected at 77 K by an ASAP2020 volumetric adsorption analyzer (Micromeritics, USA). The samples were degassed at 200 °C for 12 h before measurement. The fluorescence emission spectra of the end-capped CNPCs dispersed in various solvents were recorded with a RF-5301PC spectrometer under the excitation wavelength of 365 nm (Shimadz, Japan). The hydrodynamic diameter of the CNPCs in water was achieved using a Zetasizer Nano at 25 °C (Malvern, UK).

■ RESULTS AND DISCUSSION

Conjugated polymer colloids are emerging as viable alternatives to conventional conjugated polymers in that they have well-defined colloidal nanostructures that can be conveniently incorporated within devices by either spin-coating or inkjet printing.[13] Meanwhile, the intrinsic conductivity and luminescence of the conjugated polymers are retained, even though the polymeric chains become interpenetrated within the sterically confined micro- or nanoparticles.[14] The notoriously difficult processing of CMPs seems to be overcome to some extent by adopting the form of polymer colloids. However, we are aware that the reported conjugated polymer colloids have been nonporous and engineered with linear or ladder polymers substituted with alkyl side chains. Such one-dimensional conjugated polymers tend to preferentially intertwine or stack, and so do not provide sufficient spatial isolation upon evacuation of the solvent molecules. This leads to nonporous, compacted microstructures. Although the conventional approaches for the synthesis of polymer colloids, such as emulsion or dispersion polymerization, are equally suited for the synthesis of CMP colloids, the generation of permanent pores in heterogeneous systems, as well as definite control over the colloidal morphology of rigid networks, apparently remains unexplored.

In our work, the conjugated nanoporous polymer colloids (CNPCs) were synthesized by the polymerization of poly(*p*-phenyleneethynylene) (PPE) networks by a classical Sonogashira–Hagihara coupling reaction of terminal alkynes with aryl halides, as depicted in Figure 1a. To achieve confinement of morphology in this synthesis, the evolution of the PPE networks had to be controlled by an emulsion technique. A thermodynamically stable heterophase miniemulsion system consisting of surfactant-stabilized nanodroplets in a continuous phase was obtained by power ultrasound emulsification.[15] Each droplet can be regarded as an individual batch reactor suitable for producing nano- or submicrometer-scaled materials through a variety of polymerization reactions. Here, 1,3,5-triethynylbenzene and 1,4-dibromobenzene monomers together with the catalyst were dissolved in toluene, and an aqueous solution containing CTAB as surfactant was added to prepare a toluene-in-water pre-emulsion. Upon ultrasound emulsification, the obtained stable and homogeneous miniemulsion with a light-yellow color underwent polymerization to form a PPE network in the toluene nanodroplets. After the reaction, the as-synthesized products were readily dispersed in water, showing a latex-like appearance. The TEM image displayed in Figure 1b demonstrated the formation of uniform spherical CNPCs with a diameter of approximately 100 nm. It is surprising that the cross-linked networks had a totally rigid conformation, yet were capable of forming regular CNPCs aided by covalent chemical bonding. Dynamic light scattering (DLS) was employed to ascertain the aqueous stabilization in the presence of surfactants. Figure 1c shows the narrowly distributed histogram of the hydrodynamic diameters of the CNPCs in water, which gave an average particle size of 120 nm and a polydispersity index (PDI) of 0.076. This implies that the resultant product is, as expected, highly dispersed individually in water and is invariant in size when compared with its form in the dry state. The molecular composition of the CNPCs synthesized in the miniemulsion was verified by solid-state ^{13}C cross-polarization magic-angle spinning (CP/MAS) NMR. In Figure S1a (Supporting Information), signals are seen at δ = 131.6, 124.0, and 90.8 ppm, which can be reasonably assigned to the aromatic and acetylene carbons of the designed PPE networks, respectively.[8a]

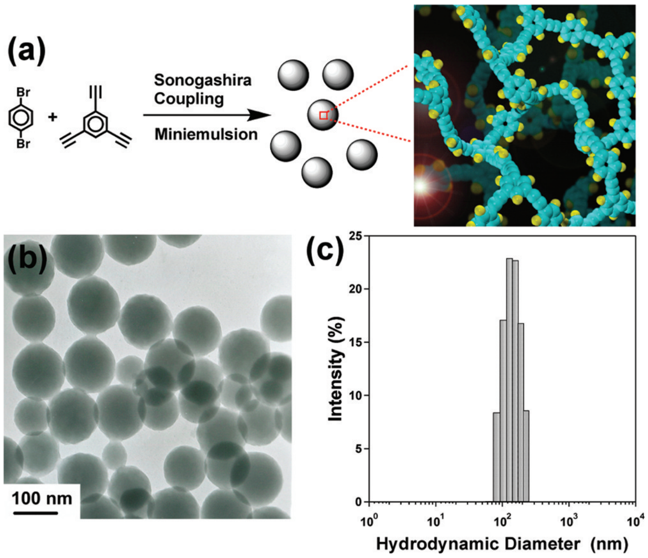

Figure 1. (a) Schematic illustration of network-inclusive CNPCs synthesized by the Sonogashira coupling reaction in a toluene-in-water miniemulsion. (b) TEM image of CNPCs. (c) Histogram of the hydrodynamic diameters of the CNPCs in aqueous solution.

Porosity was measured by means of nitrogen sorption analysis at 77 K. In Figure 2, it can be seen that the CNPCs displayed a typical type IV gas sorption isotherm, in accordance with IUPAC classification, indicative of mesoporous character. The Brunauer–Emmett–Teller (BET) model was applied to the adsorption branch, resulting in a specific surface area of 421 m^2/g and a pore volume of 0.27 cm^3/g. From a de Boer statistical thickness (*t*-plot) analysis, the CNPCs displayed a micropore contribution of 213 m^2/g (50.6%) and a mesopore

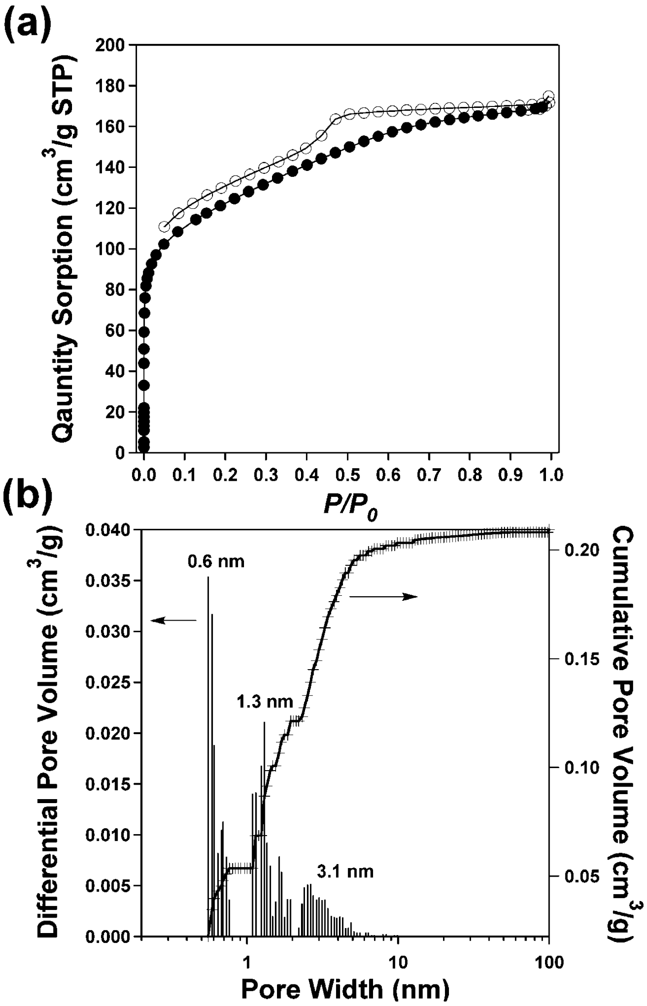

Figure 2. (a) N_2 sorption isotherm of CNPCs and (b) their pore size distribution curve calculated by the NLDFT model.

contribution of 208 m^2/g (49.4%). As compared with the similar CMP networks synthesized by Cooper et al.,[8a] the specific surface area of CNPCs was apparently lower. Also, their shapes of N_2 sorption isotherms were somewhat different, showing a significant hysteresis that was still present at low pressures. It is probably owing to a swelling of the PPE networks upon gas adsorption, which could frequently be observed in a soft network as increasing numbers of adsorbate molecules condense in the pores.[8e,16] It is assumed that the CNPC networks might have more structural defects retaining the residual nonreactive groups, and thus decrease the given surface areas. Elementary analysis in Table S1 (see the Supporting Information), showed a lower carbon content of the CNPCs than that of the similar-structured CMPs, which proves the incomplete polymerization occurring in the heterophase system. The reason may lie in that the diffusion of monomers is limited in the surfactant-confined toluene nanodroplets, and they are probably entrapped within the formed network colloids, resulting in obstruction of further evolution of the PPE networks.

The pore-size distribution was calculated by the nonlocal density functional theory (NLDFT) model and the population was found to be centered at 0.6 nm, 1.3 and 3.1 nm, respectively, as shown in Figure 2b. To the best of our knowledge, the most known CMPs have rather small pore sizes of less than 2 nm, and are thus utilized extensively to explore the capacity of gas uptake. However, mesoporosity imposed by conjugated polymer networks has rarely been considered, which is largely due to the difficulty of inhibiting the occurrence of rotation or bending imposed by the nonplanar conjugated moieties. Therefore, it is of considerable interest that the PPE network colloids display a dual distribution of nanopore sizes, which are equally populated in the mesopore and micropore ranges, respectively. Compared with the typical microporsity of the similar CMPs reported, the larger pore sizes of CNPCs might be attributed to the intrinsically defective, locked-in network that elicits a flawed pore size distribution. Besides the structural factor, it is also likely that because structural changes in measurement are not considered in evaluation of pore sizes, the typical methods just like NLDFT model might be not fully fit to determine the reliable or comparable pore size distribution.

Fabrication of CNPCs provides an important practical advantage in that the prominent optical properties of conjugated polymers are translated into a high-surface-area, dispersed, aqueous form that makes them superbly useful as sensors as a result of the possibility of enhanced three-dimensional energy migration. Before measurement, the CNPCs were subjected to an end-capping reaction with *N*-[2-(4-iodophenoxy)ethyl]-*N*,*N*-dimethylamine to remove the surfactants that might induce variations in luminescence. Solid-state ^{13}C CP/MAS NMR was used to access the molecular structure of the end-capped CNPCs. The spectrum in Figure S1b (Supporting Information) showed the expected peaks of PPE networks, corresponding to $C_{ar}{-}C$ sites at 131.6 ppm, $C_{ar}{-}H$ sites at 123.0 ppm, and sp-hybridized $-C_{ar}{-}C{\equiv}C-$ sites at 90.2 ppm. They are in agreement with those assigned in Figure S1a in the Supporting Information. The others could be well-attributed to the end-capping groups on the modified CNPCs. The peaks at 44.6 and 51.5 ppm corresponded to the $-N{-}CH_3$ and $-CH_2{-}N-$ groups. The peaks at 171.1 and 156.0 ppm could be ascribed to the $C_{ar}{-}O$ and $C_{ar}{-}H$ sites, respectively. The other types of carbon sites in the end-capping components might be overlapped by the broad peak or spinning sidebands, thereby without showing obvious lines. Elemental analysis (see Table S1 in the Supporting Information) on the modified structure showed nitrogen content of 1.46%, which was applied to determine 20.7% of the end-capping groups. Although it is possible to underestimate the nitrogen content because of the observed incomplete combustion of the sample, it still allows approximate quantification of the end-capping components.

As is evident from the fluorescence emission spectra compiled in Figure 3a, when the end-capped CNPCs were dispersed in various polar solvents, a single narrow emissive peak was observed in each case at a similar position of 450 nm, but with remarkably differential intensities. Figure 3b displays photographs of dispersions of these materials in different solvents with and without UV light irradiation (365 nm). A stable colloidal solution emitting blue fluorescence was obtained in each case, which nicely corresponded to the spectral data compiled in Figure 3a. Of more interest, the unique optical properties are unprecedented when compared with those of conventional conjugated polymers. As far as we are aware, upon transition of a PPE or its derivatives from their solution to nonsolvent conditions, the solvatochromic behavior is substantially dependent on the occurrence of aggregate-induced planarization, which elicits increased conjugation and

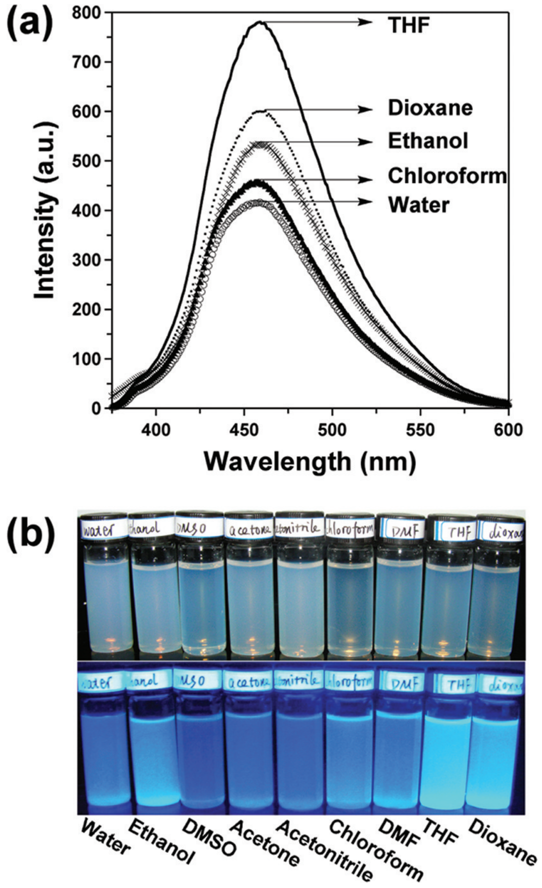

Figure 3. (a) Fluorescence emission spectrum of the CNPCs in THF, dioxane, ethanol, chloroform and water, respectively, excited with the same wavelength of 365 nm. (b) Photographs of dispersions of the CNPCs in different solvents without (up) and with (bottom) UV light irradiation (365 nm).

thus a lower band gap.[17] In sharp contrast to these previous studies, regardless of the solvent polarity, the present PPE network colloids possess single, nearly symmetrical emissive profiles, all of which resemble those of well-dissolved linear PPE chains in a good solvent. The results imply that the PPE-based CNPCs are most likely to have a chemically condensed singular microstructure, rather than being a tight agglomeration of polymeric fragments. Simultaneously, the accessible high-surface-area CNPCs allow for pronounced solvation of the conjugated moieties, leading to increased structural rigidity and hence reduced molecular rotation. As a result, the fluorescence intensity of the CNPCs was approximately doubled in THF compared to that in aqueous solution. Overall, a relatively high degree of native, solution-state, nonsolvatochromic fluorescence is obtainable, which promises attractive applicability of the CNPCs in optical sensors.

Taking into account the mesoporosity and solution properties of CNPCs, we tried to synthesize Pd nanocrystals in situ throughout the colloidal network. $Pd(OAc)_2$ in acetone was mixed with end-capped CNPCs in aqueous solution in order to complex the Pd with the ethynylene components. Thereafter, the reaction was allowed to proceed at 90 °C for 1 h for thermal decomposition of the loaded $Pd(OAc)_2$.[18] The solution turned black as the reaction progressed, whereas the acetone was removed by bubbling nitrogen through the mixture. The TEM image shown in Figure 4a confirmed that the metal nanocrystals had been embedded into the colloids. The HR TEM image in Figure 4b revealed the incorporated nanoparticles with a highly crystalline area. Together with observation of the EDX pattern in Figure S2 (see the Supporting Information), we determine that the CNPCs serve as platforms to enable the isolated dispersion of Pd nanocrystals within the network, thereby preventing the aggregation of Pd nanocrystals and their precipitation from solvents. The porosity of the Pd@CNPCs was measured to ensure the preservation of open pores derived from the organic moieties. The N_2 sorption isotherm is presented in Figure S3 (see the Supporting Information), from which it is clear that the micropores were characterized by a typical type I sorption profile. The apparent surface area and the pore volume were estimated to be 276 m^2/g and 0.15 cm^3/g, respectively, both of which are lower than previously obtained values owing to internally immobilized Pd nanocrystals. The pore-size distribution shown in the inset of Figure S3 (see the Supporting Information) was determined by employing the NLDFT model to account for the less pronounced pores with a width of 1.2 nm, which is comparable to that calculated from the microstructure of the bulk CMPs. We assume that the mesoporous components in CNPCs are filled or blocked with Pd nanocrystals so as to attain open micropores for accessibility of guest molecules.

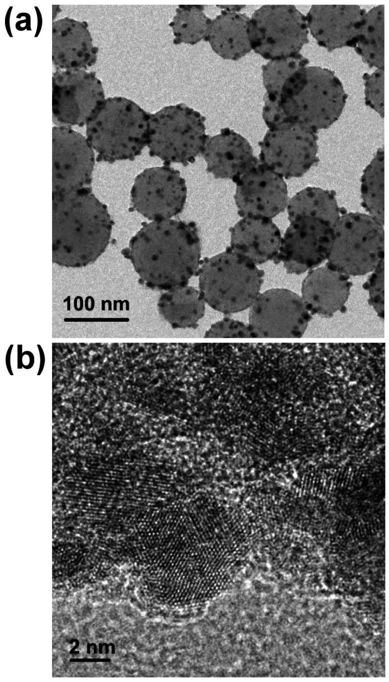

Figure 4. (a) TEM image of Pd@CNPCs and (b) HR TEM image revealing crystalline Pd nanoparticles incorporated within and attached to the CNPCs.

Table 1. Suzuki Coupling Reaction of Various Arylhalides with Phenylboronic Acid in the Presence of Pd@CNPCs.[a]

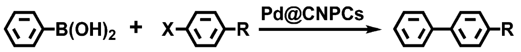

Entry	Aryl halide	Time (h)	Yield (%)[b]
1	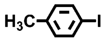	3	97.2
2	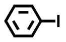	1.5	96.7
3	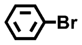	3	98.2
4	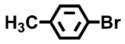	3	85.6
5	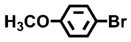	1	94.6
6	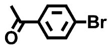	0.25	>99
7	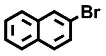	4	97.2[c]
8	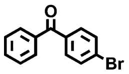	3	95.6

[a] Reaction conditions: arylhalide (1 mmol), phenylboronic acid (1.1 mmol), K_2CO_3 (1.5 mmol), Pd@CNPCs (0.1 mol %), DMF/H_2O (1.5 mL/1.5 mL), 50 °C. [b] GC yields [%]. [c] DMF/H_2O (2.5 mL/0.5 mL).

The resultant Pd@CNPCs were tested as catalysts in the Suzuki–Miyaura coupling reaction of arylboronic acids with various types of aryl halides in the presence of different bases and solvents. The as-synthesized catalyst powder was readily redispersed in polar solvents, even without any stirring, and was amenable to facile centrifugal separation from the reaction solutions. To optimize the overall process, the reaction of 1-iodo-4-methylbenzene with phenylboronic acid was selected as a model reaction that could be conveniently carried out at 50 °C. As listed in Table S2 (see the Supporting Information), the reaction did not proceed at all upon addition of CNPCs alone. Conversely, high yields of products were obtained in the presence of Pd@CNPCs. The efficiency of Pd@CNPCs containing 0.1 mol % of Pd was thoroughly investigated by varying the types of solvents and bases. Dioxane and acetonitrile proved to be poor solvents, whereas water and toluene afforded moderate yields for the same process. In sharp contrast, high activity was found in DMF, EtOH, and mixtures of either $EtOH/H_2O$ or DMF/H_2O at a 1:1 volume ratio, indicative of good suitability for the present system. Among the various bases screened in DMF/H_2O, K_2CO_3 provided the highest coupling yield of 97.2% in 3 h. As a result, the optimum

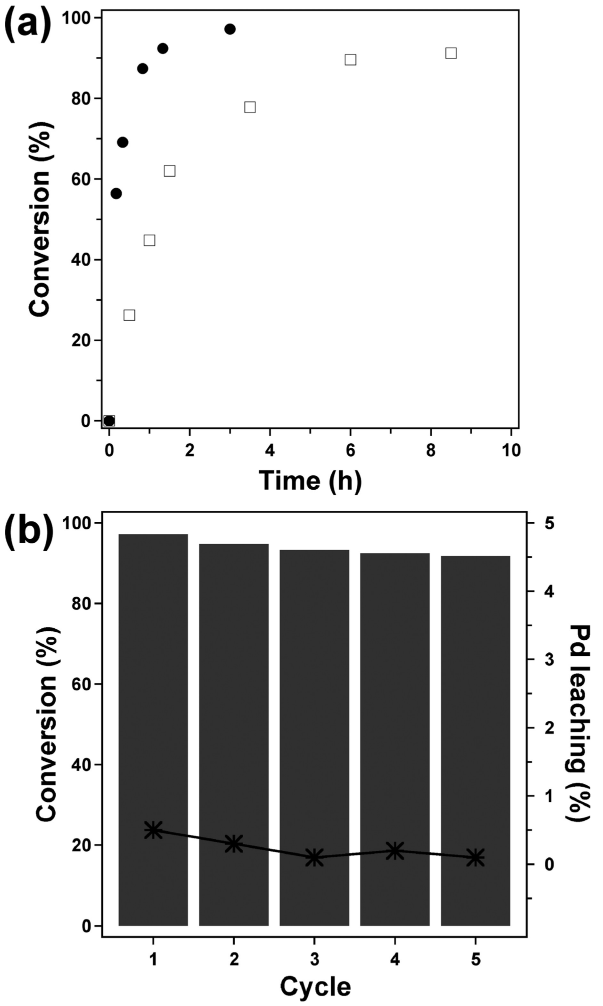

Figure 5. (a) Comparison of catalytic activity of the Pd@C (□) and Pd@CNPCs (●) catalysts in the Suzuki coupling reaction (entry 1 in Table 1). (b) Reusability of the Pd@CNPCs catalysts confirmed by both the conversions (histogram) and Pd leaching amount (−*−) in five reaction runs (entry 1 in Table 1).

conditions were attained with the Pd@CNPCs in the presence of K_2CO_3 in DMF/H_2O. We also examined the scope and limitation of the Pd@CNPCs-catalyzed cross-coupling reaction between phenylboronic acid and various iodo and bromo derivatives. All of the reactions indicated in Table 1 were completed very efficiently, giving excellent yields of the corresponding bis(aryl) products. Aryl iodides, as expected, were rapidly converted and gave high yields. Similarly, high catalytic activity was observed for the aryl bromide derivatives, regardless of the effects of electron-donating or electron-withdrawing functions. We also note that all of the reactions proceeded smoothly in relatively short times, one of which was even less than 15 min (entry 6). When the concentration of Pd was fixed at 0.1 mol %, the reaction of entry 6 was scaled-up by using 30 mmol of substrate, 33 mmol of phenylboronic acid, 45 mmol of K_2CO_3, and 0.001 mmol of catalyst, and carried out at 80 °C. The reaction proceeded rapidly and 24.5% of the aryl halide had been converted after 10 min. This resulted in a turnover number (TON) of 7350 and a turnover frequency (TOF) of 44100 h^{-1}. To the best of our knowledge, this is the highest TOF hitherto obtained for a Suzuki–Miyaura reaction with a heterogeneous catalyst. Moreover, we highlight the likelihood of a further enhancement of TOF upon lowering the Pd concentration because the activity of the catalyst is quite remarkable at low concentrations.

Commercially available Pd on charcoal (Pd@C) was used as a reference to establish an approximate activity ranking. The reaction of entry 1 in Table 1 as a test model was monitored as a function of reaction time. Using Pd@C and Pd@CNPCs with equivalent concentrations of Pd, it can be seen from Figure 5a that higher activity was achieved with Pd@CNPCs, allowing for complete conversion (97.2%) in 3 h, whereas with Pd@C, a reaction time of more than 8 h was needed to afford just 91.2% of the product. Subsequently, the reusability and recovery of Pd@CNPCs were evaluated, with particular consideration of the solid catalyst used in the reaction. For the same coupling reaction as studied above, it is evident from Figure 5b that high coupling yields were attained in all five reaction runs, accompanied by very low leaching of the Pd catalyst as determined by ICP. The results again indicate that the recoverable catalytic activity of Pd@CNPCs makes it an attractive alternative to commercially available Pd catalysts such as Pd on charcoal.

■ CONCLUDING REMARKS

To summarize, PPE-based CNPCs have been synthesized by Sonogashira coupling reaction of 1,3,5-triethynylbenzene and 1,4-dibromobenzene in a toluene-in-water miniemulsion. Polymerization was carried out with the assistance of a surfactant in the toluene nanodroplets, leading to solution-dispersible spherical nanoparticles with a relatively narrow size distribution. The resultant CNPCs retained a well-defined conjugated framework architecture, which afforded them both micro- and mesoporosity simultaneously. It is reasoned that the origin of this mesoporosity may be a surfactant-confined evolution of the PPE network in the toluene phase. The end-capped CNPCs could be dispersed in a number of solvents and emitted intense blue fluorescence in each case with the single, equally positioned, symmetrical emission profile. No solvatochromic behavior depending on forced planarization of the conjugated moieties was observed because the CNPCs were constructed entirely from three-dimensional scaffolds and did not comprise agglomerates of polymeric fragments that would easily give rise to a solvatochromic effect. Moreover, the highest intensity of fluorescence emission was found upon dispersion of the CNPCs in THF, largely due to the solvation-induced stiffness of backbones against free rotation or bending of the conjugated units. In this context, Pd nanocrystals were synthesized in situ on the end-capped CNPCs as a support, and unequivocally showed an isolated distribution of as-synthesized nanocrystals. The obtained Pd@CNPCs have been applied as an effective and reusable catalyst for the Suzuki–Miyaura coupling of a variety of haloarenes with arylboronic acids. Extraordinarily high activities with TOF up to 44 100 h^{-1} and very low leaching of the catalyst during a recycling procedure demonstrate that Pd@CNPCs are attractive as a promising alternative to commercially available Pd catalysts. We therefore speculate that this innovative system may have great potential, and opens the way for designing a variety of metal-hybrid porous materials based on the CNPCs with nano-porosity, photoluminescence properties, and conjugated scaffolds as supports.

■ ASSOCIATED CONTENT

Ⓢ Supporting Information

Synthetic procedure, solid-state ^{13}C NMR spectra, nitrogen adsorption isotherm, elementary analysis, and catalytic activity (PDF). This material is available free of charge via the Internet at http://pubs.acs.org/.

■ AUTHOR INFORMATION

Corresponding Author

*E-mail: guojia@fudan.edu.cn.

Present Address

[⊥] Department of Chemistry, University of California, Riverside, CA 92521.

Author Contributions

[‡] These authors contributed equally.

■ ACKNOWLEDGMENTS

We acknowledge the support by the National Natural Science Foundation of China (Grant 21004012), the Research Fund for the Doctoral Program of Higher Education of China (Grant 20100071120007), and the Fundamental Research Funds for the Central Universities.

■ REFERENCES

(1) (a) Ben, T.; Ren, H.; Ma, S.; Cao, D.; Lan, J.; Jing, X.; Wang, W.; Xu, J.; Deng, F.; Simmons, J. M.; Qiu, S.; Zhu, G. *Angew. Chem., Int. Ed.* **2009**, *48*, 9457. (b) Li, A.; Lu, R.-F.; Wang, Y.; Wang, X.; Han, K.-L.; Deng, W.-Q. *Angew. Chem., Int. Ed.* **2010**, *49*, 3330.

(2) (a) Chen, L.; Yang, Y.; Jiang, D. *J. Am. Chem. Soc.* **2010**, *132*, 9138. (b) Xie, Z.; Wang, C.; deKrafft, K. E.; Lin, W. *J. Am. Chem. Soc.* **2011**, *133*, 2056. (c) Jiang, J.-X.; Wang, C.; Laybourn, A.; Hasell, T.; Clowes, R.; Khimyak, Y. Z.; Xiao, J.; Higgins, S. J.; Adams, D. J.; Cooper, A. I. *Angew. Chem., Int. Ed.* **2011**, *123*, 1104. (d) Chen, L.; Yang, Y.; Guo, Z.; Jiang, D. *Adv. Mater.* **2011**, *23*, 3149.

(3) Chen, L.; Honsho, Y.; Seki, S.; Jiang, D. *J. Am. Chem. Soc.* **2010**, *132*, 6742.

(4) Kou, Y.; Xu, Y.; Guo, Z.; Jiang, D. *Angew. Chem., Int. Ed.* **2011**, *50*, 8753.

(5) Tsyurupa, M. P.; Davankov, V. A. *React. Funct. Polym.* **2006**, *66*, 768.

(6) McKeown, N. B.; Budd, P. M. *Chem. Soc. Rev.* **2006**, *35*, 675.

(7) (a) Côté, A. P.; Benin, A. I.; Ockwig, N. W.; O'Keeffe, M.; Matzger, A. J.; Yaghi, O. M. *Science* **2005**, *310*, 1166. (b) Tilford, R. W.; Gemmill, W. R.; zur Loye, H.-C.; Lavigne, J. J. *Chem. Mater.* **2006**, *18*, 5296. (c) El-Kaderi, H. M.; Hunt, J. R.; Mendoza-Cortés, J. L.; Côté, A. P.; Taylor, R. E.; O'Keeffe, M.; Yaghi, O. M. *Science* **2007**, *316*, 268. (d) Kuhn, P.; Antonietti, M.; Thomas, A. *Angew. Chem., Int. Ed.* **2008**, *47*, 3450. (e) Wan, S.; Guo, J.; Kim, J.; Ihee, H.; Jiang, D. *Angew. Chem., Int. Ed.* **2008**, *47*, 8826. (f) Campbell, N. L.; Clowes, R.; Ritchie, L. K.; Cooper, A. I. *Chem. Mater.* **2009**, *21*, 204. (g) Wan, S.; Guo, J.; Kim, J.; Ihee, H.; Jiang, D. *Angew. Chem., Int. Ed.* **2009**, *48*, 5439. (h) Bojdys, M. J.; Jeromenok, J.; Thomas, A.; Antonietti, M. *Adv. Mater.* **2010**, *22*, 2202. (i) Spitler, E. L.; Dichtel, W. R. *Nature Chem.* **2010**, *2*, 672. (j) Ding, X.; Guo, J.; Feng, X.; Honsho, Y.; Guo, J.-D.; Seki, S.; Maitarad, P.; Saeki, A.; Nagase, S.; Jiang, D. *Angew. Chem., Int. Ed.* **2011**, *50*, 1289.

(8) (a) Jiang, J.-X.; Su, F.; Trewin, A.; Wood, C. D.; Campbell, N. L.; Niu, H.; Dickinson, C.; Ganin, A. Y.; Rosseinsky, M. J.; Khimyak, Y. Z.; Cooper, A. I. *Angew. Chem., Int. Ed.* **2007**, *46*, 8574. (b) Jiang, J.-X.; Su, F.; Trewin, A.; Wood, C. D.; Niu, H.; Jones, J. T. A.; Khimyak, Y. Z.; Cooper, A. I. *J. Am. Chem. Soc.* **2008**, *130*, 7710. (c) Kuhn, P.; Forget, A.; Su, D.; Thomas, A.; Antonietti, M. *J. Am. Chem. Soc.* **2008**, *130*, 13333. (d) Kuhn, P.; Forget, A.; Hartmann, J.; Thomas, A.; Antonietti, M. *Adv. Mater.* **2008**, *21*, 897. (e) Schmidt, J.; Weber, J.; Epping, J. D.; Antonietti, M.; Thomas, A. *Adv. Mater.* **2009**, *21*, 702. (f) Cooper, A. I. *Adv. Mater.* **2009**, *21*, 1291. (g) Lu, W.; Yuan, D.; Zhao, D.; Schilling, C. I.; Plietzsch, O.; Muller, T.; Bräse, S.; Guenther, J.; Blümel, J.; Krishna, R.; Li, Z.; Zhou, H.-C. *Chem. Mater.* **2010**, *22*, 5964. (h) Pandey, P.; Katsoulidis, A. P.; Eryazici, I.; Wu, Y.; Kanatzidis, M. G.; Nguyen, S. T. *Chem. Mater.* **2010**, *22*, 4974. (i) Thomas, A. *Angew. Chem., Int. Ed.* **2010**, *49*, 8328. (j) Rabbani, M. G.; El-Kaderi, H. M. *Chem. Mater.* **2011**, *23*, 1650.

(9) Moon, S.-Y.; Bae, J.-S.; Jeon, E.; Park, J.-W. *Angew. Chem., Int. Ed.* **2010**, *49*, 9504.

(10) Chan-Thaw, C. E.; Villa, A.; Katehomol, P.; Su, D.; Thomas, A.; Prati, L. *Nano Lett.* **2010**, *10*, 537.

(11) Hasell, T.; Wood, C. D.; Clowes, R.; Jones, J. T. A.; Khimyak, Y. Z.; Adams, D. J.; Cooper, A. I. *Chem. Mater.* **2010**, *22*, 557.

(12) Weder, C. *Chem. Commun.* **2005**, 5378.

(13) Pecher, J.; Mecking, S. *Chem. Rev.* **2010**, *110*, 6260.

(14) (a) Hittinger, E.; Kokil, A.; Weder, C. *Angew. Chem., Int. Ed.* **2004**, *43*, 1808. (b) Baier, M. C.; Huber, J.; Mecking, S. *J. Am. Chem. Soc.* **2009**, *131*, 14267.

(15) Antonietti, M.; Landfester, K. *Prog. Polym. Sci.* **2002**, *27*, 689.

(16) (a) Weber, J.; Antonietti, M.; Thomas, A. *Macromolecules* **2008**, *41*, 2880. (b) Weber, J.; Thomas, A. *J. Am. Chem. Soc.* **2008**, *130*, 6334.

(17) Bunz, U. H. F. *Macromol. Rapid Commun.* **2009**, *30*, 772.

(18) Ohtaka, A.; Teratani, T.; Fujii, R.; Ikeshita, K.; Shimomura, O.; Nomura, R. *Chem. Commun.* **2009**, 7188.